

NATURAL-MODE REPRESENTATION FOR THE FIELD REFLECTED BY AN INHOMOGENEOUS CONDUCTOR-BACKED MATERIAL LAYER – TE CASE

E. J. Rothwell

Department of Electrical and Computer Engineering
Michigan State University
East Lansing, MI, 48824, USA

Abstract—The transient plane-wave field reflected by a conductor-backed, inhomogeneous, planar material layer is considered. The reflected field is written as a natural-mode expansion, and the natural resonance frequencies of the slab are found by solving a homogeneous integral equation for the field within the slab. Several examples are considered, and the natural mode series is verified by comparison to the inverse fast-Fourier transform of the frequency-domain reflected field.

1. INTRODUCTION

The probing of material layers using transient electromagnetic fields has received extensive study, with applications to fault detection and material parameters extraction. Using the transient reflected field, the material profile of inhomogeneous planarly-layered materials may be reconstructed [1–6]. In a related application, it may only be important to determine whether the properties of layered materials have changed due to environmental degradation or misapplication. Because the reflected field consists of multiple reflections of waves within the layers, it may be possible to write the reflection coefficient as a natural mode series, and use the E-pulse technique to determine whether the resonance frequencies, and thus the material properties, have changed [7].

It has been shown previously that the transient field reflected by a simple, lossy, conductor-backed layer [8], and also by a conductor-backed layer of Debye material [9], can be written as a natural mode series. It has also been shown that a conductor-backed stack of simple lossy materials may be written in terms of natural modes [10]. In

many situations the materials are comprised of inhomogeneous layers, and thus it is of interest to investigate whether the field reflected by a conductor-backed inhomogeneous layer may be written as a natural mode series.

Tijhuis and Blok analyzed the transient field reflected and transmitted by an inhomogeneous slab of dielectric material [11]. They found that, under the conditions of their problem, the transient field could be described using natural modes. However, they only considered normal incidence, and very specific excitation signals. In the present study, the obliquely-incident plane-wave impulse response of an inhomogeneous conductor-backed layer is considered. Inhomogeneities in both the permittivity and permeability are examined, and comparison is made to exact frequency-domain solutions for specific material profiles. Finally, the natural frequencies of several inhomogeneous layers are found, and the late-time reflected field is constructed as a natural-mode series and compared to the inverse fast-Fourier transform of the theoretical frequency-domain solution.

2. DIFFERENTIAL EQUATION FOR THE FIELD

A plane wave with its electric field polarized in the y-direction (TE polarization) is incident from free space onto an interface between free space and a conductor-backed material layer. The material layer has thickness d , and complex inhomogeneous material parameters $\epsilon(z, \omega) = \epsilon_0 \epsilon_r(z, \omega)$, $\mu(z, \omega) = \mu_0 \mu_r(z, \omega)$, and $\sigma(z, \omega)$. The electric field in region 0 ($z < 0$) or in region 1 ($z > 0$) may be written as $\vec{E}(x, z, \omega) = \hat{y}E_y(x, z, \omega)$. From Faraday's law, the magnetic field is given by

$$\vec{H}(x, z, \omega) = \frac{j}{\omega\mu(z, \omega)} \left[-\hat{x} \frac{\partial E_y(x, z, \omega)}{\partial z} + \hat{z} \frac{\partial E_y(x, z, \omega)}{\partial x} \right]. \quad (1)$$

Substituting this into Ampere's law yields the differential equation

$$\left(\frac{\partial^2}{\partial x^2} + \frac{\partial^2}{\partial z^2} - \frac{1}{\mu(z, \omega)} \frac{\partial \mu(z, \omega)}{\partial z} \frac{\partial}{\partial z} + k^2(z, \omega) \right) E_y(x, z, \omega) = 0 \quad (2)$$

where $k(z, \omega) = \omega \sqrt{\mu(z, \omega) \epsilon_c(z, \omega)}$ is the wavenumber, with $\epsilon_c(z, \omega) = \epsilon(z, \omega) - j\sigma(z, \omega)/\omega$ the complex permittivity.

Assume that (2) has the product solution $E_y(x, z, \omega) = f(x, \omega)g(z, \omega)$. Substitution produces the separated ordinary

differential equations

$$\frac{\partial^2 f(x, \omega)}{\partial x^2} + k_x^2(\omega) f(x, \omega) = 0 \quad (3)$$

$$\frac{\partial^2 g(z, \omega)}{\partial z^2} - \frac{1}{\mu(z, \omega)} \frac{\partial \mu(z, \omega)}{\partial z} \frac{\partial g(z, \omega)}{\partial z} + k_z^2(z, \omega) g(z, \omega) = 0 \quad (4)$$

where $k_z^2(z, \omega) = k^2(z, \omega) - k_x^2(\omega)$. The solution to (3) is

$$f(x, \omega) = e^{-jk_x(\omega)x} \quad (5)$$

and so $E_y(x, z, \omega) = e^{-jk_x(\omega)x} g(z, \omega)$. In region 0, $k_x(\omega) = k_{x0}(\omega) = k_0(\omega) \sin \phi_0$, where ϕ_0 is the angle of incidence measured from the normal to the interface, and $k_0(\omega) = \omega \sqrt{\mu_0 \epsilon_0}$. Also, in this region there will be two waves, one associated with the incident field and one with the reflected field. The solution to (4) in region 0 is $g(z, \omega) = E_0(\omega) e^{-jk_{z0}z}$ for the incident wave, where $k_{z0}(\omega) = [k_0^2(\omega) - k_x^2(\omega)]^{1/2} = k_0(\omega) \cos \phi_0$, and $g(z, \omega) = E_r(\omega) e^{jk_{z0}z}$ for the reflected wave. Thus, the total electric field in region 0 is

$$E_y(x, z, \omega) = E_0(\omega) e^{-jk_{x0}(\omega)x} e^{-jk_{z0}(\omega)z} + E_r(\omega) e^{-jk_{x0}(\omega)x} e^{jk_{z0}(\omega)z}. \quad (6)$$

Using (1), H_x in region 0 is

$$\begin{aligned} H_x(x, z, \omega) = & -\frac{\cos \phi_0}{\eta_0} E_0(\omega) e^{-jk_{x0}(\omega)x} e^{-jk_{z0}(\omega)z} \\ & + \frac{\cos \phi_0}{\eta_0} E_r(\omega) e^{-jk_{x0}(\omega)x} e^{jk_{z0}(\omega)z}. \end{aligned} \quad (7)$$

In region 1, k_x must take on the same value as in region 0 in order to satisfy the boundary conditions on tangential fields at $z = 0$. Thus, the *total* electric field (sum of forward and reverse traveling waves) in region 1 is

$$E_y(x, z, \omega) = g(z, \omega) e^{-jk_{x0}(\omega)x}, \quad (8)$$

while the total x-directed magnetic field is

$$H_x(x, z, \omega) = \frac{-j}{\omega \mu(z, \omega)} e^{-jk_{x0}(\omega)x} \frac{\partial g(z, \omega)}{\partial z}. \quad (9)$$

The boundary relations required to solve (4) may be found using the jump conditions on the tangential fields. Setting $E_y = 0$ on the

surface of the conductor gives $g(d, \omega) = 0$. Enforcing continuity of tangential \vec{E} and \vec{H} at $z = 0$ gives, respectively,

$$E_0(\omega) + E_r(\omega) = g(0, \omega) \quad (10)$$

$$-E_0(\omega) + E_r(\omega) = -j \frac{\eta_0}{\cos \phi_0} \frac{1}{\omega \mu(0, \omega)} \frac{\partial g(z, \omega)}{\partial z} \Big|_{z=0}. \quad (11)$$

Equations (10) and (11) may be subtracted to give the two boundary conditions

$$2E_0(\omega) = g(0, \omega) + a(\omega) \frac{\partial g(z, \omega)}{\partial z} \Big|_{z=0}, \quad (12)$$

$$g(d, \omega) = 0, \quad (13)$$

where $a(\omega) = j\eta_0/[\omega\mu(0, \omega) \cos \phi_0]$.

3. SOLUTION TO THE DIFFERENTIAL EQUATION

Assume that the quantity $k_z^2(z, \omega)$ is continuous on $(0, d)$, or is continuous within a finite number of subintervals with discontinuities on the boundaries of the subintervals (the multiple region problem). Then, the second-order differential equation (4) has two independent fundamental solutions, $g_1(z, \omega)$ and $g_2(z, \omega)$. Thus,

$$g(z, \omega) = A_1(\omega)g_1(z, \omega) + A_2(\omega)g_2(z, \omega), \quad (14)$$

where A_1 and A_2 are determined by the boundary conditions. Applying (12) and (13) gives

$$g(z, \omega) = \frac{2E_0(\omega)}{F(\omega) + a(\omega)G(\omega)} [g_2(d, \omega)g_1(z, \omega) - g_1(d, \omega)g_2(z, \omega)], \quad (15)$$

where

$$F(\omega) = g_1(0, \omega)g_2(d, \omega) - g_1(d, \omega)g_2(0, \omega), \quad (16)$$

$$G(\omega) = g_1'(0, \omega)g_2(d, \omega) - g_1(d, \omega)g_2'(0, \omega), \quad (17)$$

with $g_1'(z, \omega) = \partial g_1(z, \omega)/\partial z$, etc.

The reflection coefficient for the reflected field in region 0 is defined as $\Gamma(\omega) = E_r(\omega)/E_0(\omega)$, which, from (10), may be written as

$$\Gamma(\omega) = -1 + \frac{1}{E_0(\omega)} g(0, \omega). \quad (18)$$

Substituting from (15) gives

$$\Gamma(\omega) = \frac{F(\omega) - a(\omega)G(\omega)}{F(\omega) + a(\omega)G(\omega)}. \quad (19)$$

As a simple example, consider a material layer with uniform conductivity $\sigma(\omega)$, uniform permeability $\mu(z, \omega) = \mu_r(\omega)\mu_0$ and uniform permittivity $\epsilon(z, \omega) = \epsilon_r(\omega)\epsilon_0$. Then, the differential equation (4) becomes

$$\frac{\partial^2 g(z, \omega)}{\partial z^2} + k_z^2(\omega)g(z, \omega) = 0. \quad (20)$$

This has the solutions $g_1 = \sin k_z z$ and $g_2 = \cos k_z z$. Substituting into (15) gives the solution

$$g(z, \omega) = 2E_0(\omega) \frac{\sin k_z(d - z)}{\sin k_z d - ja \cos k_z d}. \quad (21)$$

The reflection coefficient (18) may then be written as

$$\Gamma(\omega) = \frac{\Gamma_0 - P^2}{1 - \Gamma_0 P^2} \quad (22)$$

where $P = e^{-jk_z d}$ and

$$\Gamma_0 = \frac{1 - a}{1 + a} = \frac{\mu_r \cos \phi_0 - \sqrt{\mu_r \epsilon_r - \sin^2 \phi_0}}{\mu_r \cos \phi_0 + \sqrt{\mu_r \epsilon_r - \sin^2 \phi_0}} \quad (23)$$

is the interfacial reflection coefficient. Equation (22) is the well-known result for a conductor-backed homogeneous layer [8].

As a second example, consider a material layer with zero conductivity, homogeneous permeability $\mu(z, \omega) = \mu_r(\omega)\mu_0$, and an exponential permittivity profile

$$\epsilon(z, \omega) = \epsilon_{r0}(\omega)\epsilon_0 e^{\kappa(\omega)z}. \quad (24)$$

Then, the differential equation (4) becomes

$$\frac{\partial^2 g(z, \omega)}{\partial z^2} + [k_0^2 \mu_r(\omega) \epsilon_{r0}(\omega) e^{\kappa(\omega)z} - k_x^2(\omega)] g(z, \omega) = 0. \quad (25)$$

This equation has the form $w''(z) + (\lambda^2 e^{2z} - \nu^2)w(z) = 0$, which has the solution given by equation (9.1.54) of [12]: $w(z) = C_\nu(\lambda e^z)$, where

$C_\nu(z)$ is any ordinary Bessel function of order ν . Using this, the differential equation (25) has the solutions

$$g_1(z, \omega) = J_\nu(\lambda e^{\kappa z/2}), \quad g_2(z, \omega) = Y_\nu(\lambda e^{\kappa z/2}), \quad (26)$$

where $\lambda = 2k_0\sqrt{\mu_r\epsilon_{r0}}/\kappa$ and $\nu = 2k_x/\kappa$.

For a third example, consider a material layer with zero conductivity, homogeneous permittivity $\epsilon(z, \omega) = \epsilon_r(\omega)\epsilon_0$, and an exponential permeability profile

$$\mu(z, \omega) = \mu_{r0}(\omega)\mu_0 e^{\kappa(\omega)z}. \quad (27)$$

Then, the differential equation (4) becomes

$$\frac{\partial^2 g(z, \omega)}{\partial z^2} - \kappa(\omega) \frac{\partial g(z, \omega)}{\partial z} + [k_0^2 \epsilon_r(\omega) \mu_{r0}(\omega) e^{\kappa(\omega)z} - k_x^2(\omega)] g(z, \omega) = 0. \quad (28)$$

This differential equation takes the form $g'' - \kappa g' + (Ae^{\kappa z} - k_x^2)g = 0$, where $A = k_0^2 \epsilon_r \mu_{r0}$. Using the substitution $u^2 = Ae^{\kappa z}$ then gives the differential equation

$$\frac{\partial^2 g(u)}{\partial u^2} - \frac{1}{u} \frac{\partial g(u)}{\partial u} + \left[\left(\frac{2}{\kappa}\right)^2 - \frac{\left(\frac{2}{\kappa}\right)^2 k_x^2}{u^2} \right] g(u) = 0. \quad (29)$$

The solution to this equation is given in equation (8.491.6) of [13]. Substituting for u in terms of z into that solution results in the solution to (28):

$$g_1 = e^{\kappa z/2} J_\nu(\lambda e^{\kappa z/2}), \quad g_2 = e^{\kappa z/2} Y_\nu(\lambda e^{\kappa z/2}) \quad (30)$$

where $\lambda = 2k_0\sqrt{\epsilon_r\mu_{r0}}/\kappa$ and $\nu = \sqrt{1 + (2k_x/\kappa)^2}$.

4. CONVERSION TO AN INTEGRAL EQUATION

In most cases an analytical solution to the differential equation (4) is not available. Then, the differential equation must be solved numerically [14]. Alternatively, the differential equation may be converted into an integral equation. This latter approach is appealing due to the ease of solving the resulting integral equation and determining the natural resonance frequencies of the structure.

The differential equation (4) may be written in the form

$$g''(z) + h(z)g'(z) + f(z)g(z) = 0 \quad (31)$$

where $f(z) = k_z(z)$ and $h(z) = -\mu'(z)/\mu(z)$. An integral equation for $g(z)$ is obtained by integrating (31) twice. The first integration gives

$$g'(z) + \int_0^z h(t)g'(t) dt + \int_0^z f(t)g(t) dt = C_1. \quad (32)$$

When $\mu(z)$ is twice differentiable, integration by parts may be used on the second term to yield

$$g'(z) + h(z)g(z) + \int_0^z [f(t) - h'(t)] g(t) dt = C_1. \quad (33)$$

A second integration then gives

$$g(z) = - \int_0^z h(t)g(t) dt - \int_0^z (z-t) [f(t) - h'(t)] g(t) dt + C_1z + C_2. \quad (34)$$

The constants C_1 and C_2 are evaluated by applying the boundary conditions (12) and (13). This results in

$$g(z) = - \int_0^z \{h(t) + (z-t) [f(t) - h'(t)]\} g(t) dt + \frac{a-zh_0}{a-dh_0} \int_0^d \{h(t) + (d-t) [f(t) - h'(t)]\} g(t) dt + 2E_0 \frac{z-d}{a-dh_0}, \quad (35)$$

where $h_0 = 1 - ah(0)$. This is a mixed-type integral equation for $g(z)$.

An alternative integral equation may be obtained by integrating (32) to give

$$g(z) + \int_0^z (z-t) [f(t)g(t) + h(t)g'(t)] dt = C_1z + C_2. \quad (36)$$

Applying the boundary conditions (12) and (13) gives

$$g(z) = \int_0^d \left[\frac{a-zh_0}{a-dh_0} (d-t) - (z-t)u(z-t) \right] [f(t)g(t) + h(t)g'(t)] dt + 2E_0 \frac{z-d}{a-dh_0} \quad (37)$$

where $u(z)$ is the unit step function. This is an integro-differential equation for $g(z)$.

Under the condition that $h(z) = \mu'(z)/\mu(z) = 0$ (uniform permeability), both (35) and (37) reduce to the simpler integral equation

$$g(z) = \int_0^d \left[\frac{a-zh_0}{a-dh_0} (d-t) - (z-t)u(z-t) \right] f(t)g(t) dt + 2E_0 \frac{z-d}{a-dh_0} \quad (38)$$

with $h_0 = 1$.

Any of the integral equations (35), (37), or (38) may be solved using the method of moments. Both collocation (rectangular pulse function expansion with point matching) and Galerkin's method with continuous basis functions have been used successfully to solve for $g(z)$, which is a continuous function even when $f(z)$ is discontinuous. As an example, applying Galerkin's method to (38) using the expansion

$$g(z) = \sum_{n=1}^N a_n g_n(z) \quad (39)$$

produces the matrix equation

$$[A_{mn}] a_n = f_m \quad (40)$$

where

$$A_{mn} = W_{mn} + U_{mn} - G_m H_n \quad (41)$$

with

$$W_{mn} = \int_0^d g_m(z) g_n(z) dz \quad (42)$$

$$U_{mn} = \int_0^d g_m(z) \left[\int_0^z (z-t) f(t) g_n(t) dt \right] dz \quad (43)$$

$$G_m = \int_0^d g_m(z) \frac{a - zh_0}{a - dh_0} dz \quad (44)$$

$$H_n = \int_0^d g_n(t) (d-t) f(t) dt \quad (45)$$

$$f_m = \frac{2E_0}{a - dh_0} \int_0^d g_m(z) (z-d) dz, \quad (46)$$

where $h_0 = 1$. Using, instead, collocation by partitioning the layer into N partitions of width Δ and point matching at the centers of the partitions leads again to matrix equation (40), but with

$$A_{mn} = \delta_{mn} + U_{mn} - V_{mn}, \quad (47)$$

where

$$U_{mn} = \begin{cases} 0, & m < n \\ \int_{(m-1)\Delta}^{(m-1/2)\Delta} (z_m - t) f(t) dt, & m = n \\ \int_{(n-1)\Delta}^{n\Delta} (z_m - t) f(t) dt, & m > n \end{cases} \quad (48)$$

$$V_{mn} = \frac{a - z_m h_0}{a - d h_0} \int_{(n-1)\Delta}^{n\Delta} (d - t) f(t) dt \quad (49)$$

$$f_m = 2E_0 \frac{z_m - d}{a - d h_0}. \quad (50)$$

Here $z_m = (m - 1/2)\Delta$ and δ_{mn} is the Kronecker delta function.

As a second example, consider the form of (35) under the assumption of an exponential permeability profile, $\mu(z) = \mu_{r0}\mu_0 e^{\kappa z}$:

$$g(z) + \int_0^z \{-\kappa + (z - t)f(t)\} g(t) dt - \frac{a - z h_0}{a - d h_0} \int_0^d \{-\kappa + (d - t)f(t)\} g(t) dt = 2E_0 \frac{z - d}{a - d h_0}, \quad (51)$$

where $h_0 = 1 + a\kappa$. Using Galerkin's method with the expansion (39) gives the matrix equation (40) with the entries

$$A_{mn} = W_{mn} - \kappa Q_{mn} + U_{mn} + \kappa G_m S_n - G_m H_n. \quad (52)$$

Here W_{mn} , U_{mn} , G_m , H_n , and f_m are given in (42)-(46), while

$$S_n = \int_0^d g_n(t) dt \quad (53)$$

$$Q_{mn} = \int_0^d g_m(z) \left[\int_0^z g_n(t) dt \right] dz. \quad (54)$$

If collocation is used on (51) instead, the matrix entries are given by

$$A_{mn} = \delta_{mn} - \kappa Y_{mn} + U_{mn} + \kappa \Delta T_m - V_{mn}. \quad (55)$$

Here U_{mn} , V_{mn} , and f_m are given in (48)-(50), while

$$T_m = \frac{a - z_m h_0}{a - d h_0} \quad (56)$$

$$Y_{mn} = \begin{cases} 0, & m < n \\ \Delta/2, & m = n \\ \Delta, & m > n. \end{cases} \quad (57)$$

As an example of solving the integral equation, consider a conductor-backed layer with two distinct homogeneous regions. Region 1 extends from $z = 0$ to $z = 0.03$ m, and has zero conductivity, unit relative permittivity, and a frequency-independent relative permeability of 4. Region 2 extends from $z = 0.03$ m to $z = 0.05$ m, has unit relative permeability, a frequency-constant conductivity of

$\sigma = 0.5 \text{ S/m}$, and a frequency-independent dielectric constant of $\epsilon' = 8$. Thus, the complex permittivity is $\epsilon(\omega) = \epsilon_0 \epsilon' - j\sigma/\omega$. The field within the layer may be obtained analytically by solving (4) for $g(z)$ in each region and applying boundary conditions (or using standard layered-medium theory as in [15, 16]). Taking the two regions as a single layer, $g(z)$ may also be found by solving (38) using Galerkin's method. A convenient choice for the expansion of $g(z)$ is as a Fourier series

$$g(z) = \sum_{n=1}^N a_n \sin \frac{n\pi}{2d}(z - d). \quad (58)$$

Note that each basis function in this expansion incorporates the boundary condition of zero electric field at $z = d$. Note also that each of the entries (41) in the matrix equation may be computed in closed form. Solving the matrix equation (40) at $f = 10 \text{ GHz}$ with $\phi_0 = 30^\circ$ produces the results for $g(z)$ shown in Figure 1. To obtain these results, 400 basis functions were used in the expansion (58). This produces an accuracy of four digits in the reflection coefficient Γ computed using (18), as compared to the analytic result ($\Gamma = 0.3470 - j0.2292$). The boundary between the two regions can be easily seen in the solution. Note that since region 2 is lossy, the amplitude of the field in that region decays with increasing z .

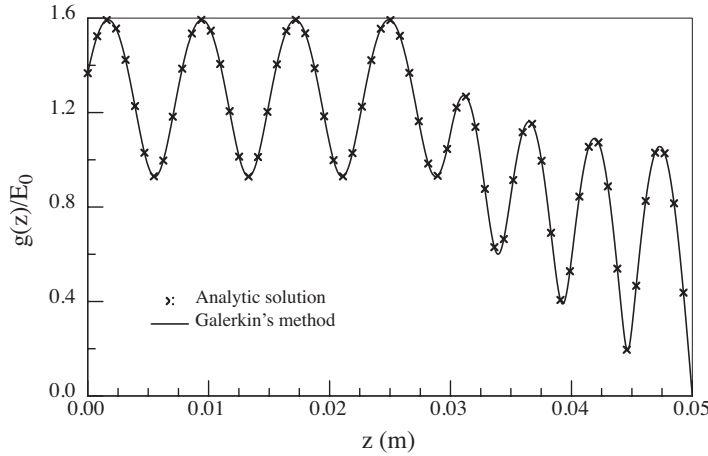


Figure 1. Magnitude of the electric field reflected by a conductor-backed layer with two homogeneous regions.

As a second example, consider a conductor-backed layer of thickness 0.03 m with zero conductivity, unit relative permeability, and

a frequency-independent exponential permittivity profile (24). The field within the layer may be found analytically by substituting (26) into (15), or numerically by solving the integral equation (38). Figure 2 compares the analytic solution to the solution of the integral equation found using collocation at $f = 10$ GHz, with $\phi_0 = 30^\circ$ and 2000 pulse basis functions. Here the frequency-independent permittivity parameters $\epsilon_{r0} = 4$ and $\kappa = 20$ were used. The number of basis functions was chosen to produce an accuracy of four digits in the reflection coefficient Γ computed numerically using (18), as compared to the analytic result ($\Gamma = 0.7368 - j0.6761$). Note that significantly more basis functions are required when using collocation than when using Galerkin's method with Fourier sine basis functions. Note also that each of the entries (47) in the matrix equation may be computed in closed form. It can be seen that the wavelength of the field decreases with increasing z , as the permittivity increases according to (24).

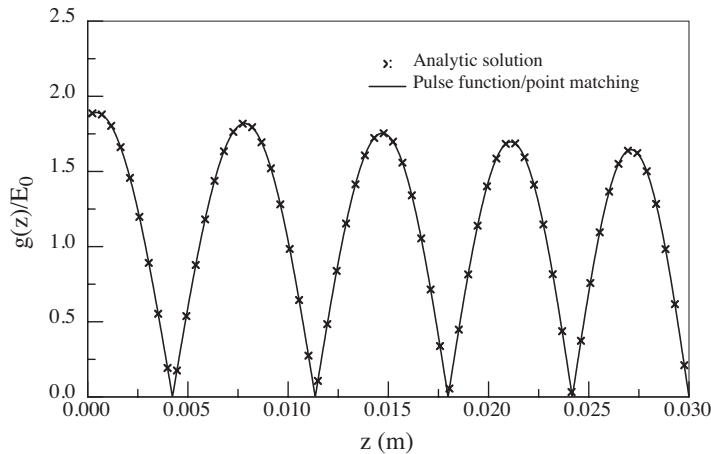


Figure 2. Magnitude of the electric field reflected by a conductor-backed layer with exponential permittivity profile.

For a third example, consider a conductor-backed layer of thickness 0.03 m with zero conductivity, unit relative permittivity, and a frequency-independent exponential permeability profile (27). The field within the layer may be found analytically by substituting (30) into (15), or numerically by solving the integral equation (51). Figure 3 compares the analytic solution to the solution of the integral equation found using collocation at $f = 10$ GHz, with $\phi_0 = 30^\circ$ and 2000 pulse basis functions. Here the frequency-independent permeability parameters $\mu_{r0} = 4$ and $\kappa = 20$ were used. The number of basis

functions was chosen to produce an accuracy of four digits in the reflection coefficient Γ computed numerically using (18), as compared to the analytic result ($\Gamma = 0.9764 - j0.2159$). Note that each of the entries (55) in the matrix equation may be computed in closed form. It can be seen that the wavelength of the field decreases with increasing z , as the permeability increases according to (27), and that the amplitude of the field increases with increasing z because of the multiplicative exponential terms in (30).

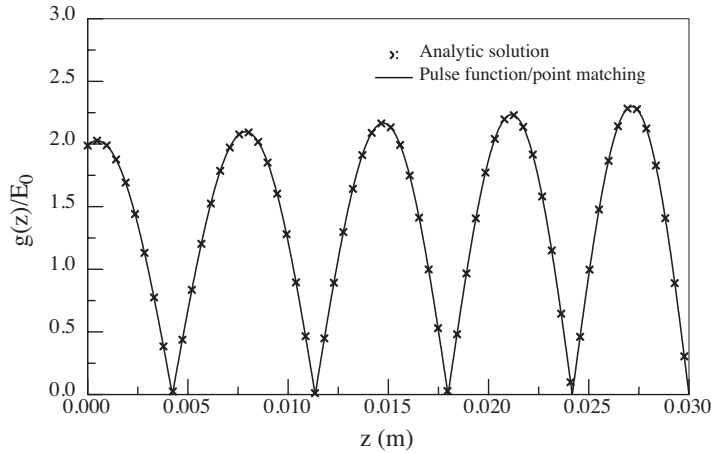


Figure 3. Magnitude of the electric field reflected by a conductor-backed layer with exponential permeability profile.

5. NATURAL-MODE EXPANSION OF THE FIELD

The solution to the integral equations gives the field within the inhomogeneous layer as a function of frequency ω . This may be extended into the complex Laplace domain by the substitution $s = j\omega$. The time-domain field is then obtained using the inverse Laplace transform.

The presence of the layer boundaries suggests that the temporal field may be written in terms of multiple reflections of waves within the layer. The singularity expansion method (SEM) [17] suggests that the Laplace-domain field may be represented as a pole series augmented by an entire function

$$g(z, s) = \sum_{n=1}^N C_n(s) \frac{e_n(z)}{s - s_n} + W(z, s). \quad (59)$$

Here s_n is the complex resonance frequency of the n^{th} mode, $e_n(z)$ is the modal field of the n^{th} mode, and $C_n(s)$ is a coupling coefficient describing how strongly the incident field couples into a particular modal field. The SEM expansion (59) may be substituted into any of the integral equations (35), (37), or (38) to obtain a homogeneous integral equation for the modal fields and natural frequencies. For example, substituting into (38) yields

$$\begin{aligned} & \sum_{n=1}^N \frac{C_n(s)}{s - s_n} \left[e_n(z) + \int_0^z (z-t)e_n(t)f(t,s)dt - \right. \\ & \qquad \qquad \qquad \left. \frac{a(s) - z}{a(s) - d} \int_0^d e_n(t)(d-t)f(t,s)dt \right] \\ & + W(z,s) \\ & + \int_0^z (z-t)f(t,s)W(t,s)dt - \frac{a(s) - z}{a(s) - d} \int_0^d W(t,s)(d-t)f(t,s)dt \\ & = 2E_0 \frac{z-d}{a(s) - d}. \end{aligned} \quad (60)$$

Multiplying both sides of this equation by $(s - s_k)$ and taking the limit as $s \rightarrow s_k$ then produces the homogeneous integral equation

$$e_k(z) + \int_0^z (z-t)e_k(t)f(t,s_k)dt - \frac{a(s_k) - z}{a(s_k) - d} \int_0^d e_k(t)(d-t)f(t,s_k)dt = 0 \quad (61)$$

When this equation is solved using the moment method (either Galerkin's method or collocation), the following matrix equation results:

$$[A_{mn}(s_k)] a_n = 0. \quad (62)$$

Since this equation is homogeneous, nontrivial solutions are only possible when

$$\det [A_{mn}(s_k)] = 0. \quad (63)$$

Equation (63) defines the natural frequencies s_k . With these, the modal fields may be found using the nullspace of the matrix equation.

6. NATURAL MODE SERIES FOR REFLECTION COEFFICIENT

It is the reflected field that is available when a material layer is interrogated. Thus, a modal series representation of the reflection

coefficient $\Gamma(s)$ is desired. From (18), the Laplace domain reflection coefficient is

$$\Gamma(s) = \frac{g(0, s)}{E_0(s)} - 1. \quad (64)$$

Substituting from (59), the natural-mode expansion of the reflection coefficient is

$$\Gamma(s) = \sum_{n=1}^N \frac{c_n}{s - s_n} + w(s) \quad (65)$$

where the natural frequencies s_n are the solutions to (63). Multiplying both sides of this expression by $(s - s_k)$ and taking the limit as $s \rightarrow s_k$, the coupling coefficient for the k^{th} mode is found as

$$c_k = \lim_{s \rightarrow s_k} (s - s_k) \Gamma(s). \quad (66)$$

Here $\Gamma(s)$ is computed from (64), using $g(0, s)$ from the solution to one of the integral equations (35), (37), or (38).

The limit in (66) may be difficult to compute numerically. An alternative method for finding the coupling coefficient is to use contour integration. Let L_k be a closed contour in the complex s -plane that encompasses the pole s_k but no other poles. Integrating (65) along L_k in the counter-clockwise direction gives

$$\oint_{L_k} \Gamma(s) ds = \sum_{n=1}^N c_n \oint_{L_k} \frac{ds}{s - s_n} + \oint_{L_k} w(s) ds. \quad (67)$$

The second integral on the right-hand side is zero by Cauchy's integral theorem. By Cauchy's residue theorem, only the k^{th} term in the series is non-zero. Thus

$$c_m = \frac{1}{2\pi j} \oint_{L_m} \Gamma(s) ds. \quad (68)$$

For the special case that L_m is a circle of radius δ centered on s_m this gives

$$c_m = \frac{\delta}{2\pi} \int_0^{2\pi} \Gamma(s_m + \delta e^{j\phi}) e^{j\phi} d\phi. \quad (69)$$

7. EXAMPLES

As a first simple example, consider a conductor-backed layer with zero conductivity, uniform frequency-independent permeability $\mu = \mu_r \mu_0$, and uniform frequency-independent permittivity $\epsilon = \epsilon_r \epsilon_0$. The natural

frequencies of the system are the poles of the reflection coefficient (22). Setting the denominator of that expression to zero gives

$$\Gamma_0 e^{-s\chi} = 1 \quad (70)$$

where

$$\chi = \frac{2d}{c} \sqrt{\mu_r \epsilon_r - \sin^2 \phi_0} \quad (71)$$

with Γ_0 given by (23) and c the speed of light in free space. When $\Gamma_0 < 0$ (true, for instance, when $\mu_r = 1$), (70) is satisfied by

$$s_n = \frac{1}{\chi} \ln |\Gamma_0| + j(2n+1) \frac{\pi}{\chi}, \quad n = 0, 1, 2, \dots \quad (72)$$

When $\Gamma_0 > 0$, (70) is satisfied by

$$s_n = \frac{1}{\chi} \ln \Gamma_0 + j2n \frac{\pi}{\chi}, \quad n = 1, 2, \dots \quad (73)$$

The coupling coefficients are found from (66) as

$$c_m = \frac{\Gamma_0 - e^{-s_m \chi}}{\frac{\partial}{\partial s} [1 - \Gamma_0 e^{-s\chi}] |_{s=s_m}} = \frac{\Gamma_0^2 - 1}{\Gamma_0 \chi}. \quad (74)$$

As a specific case, let $\mu_r = 1$, $\epsilon_r = 9$, $d = 0.1$ m, and $\phi_0 = 30^\circ$. The natural frequencies from (72) are $s_n = -3.0567 \times 10^8 + j(2n+1)1.5920 \times 10^9$ 1/s, while the coupling coefficients are found from (74) as $c_n = 6.4908 \times 10^8$ 1/s. Solving the equation (63) using collocation produces natural frequencies identical to these, with 500 basis functions required to achieve 5 digits of accuracy up to $n = 10$. Computing the coupling coefficients using (69) also produces values accurate to 5 digits.

As a second example, consider a conductor-backed layer of thickness 0.03 m with zero conductivity, unit relative permeability, and a frequency-independent exponential permittivity profile (24), where $\epsilon_{r0} = 4$ and $\kappa = 20$. The reflection coefficient is computed at 2048 points in the frequency range 0.01–20.48 GHz, by using the analytic solution to the differential equation (19) with $\phi_0 = 30^\circ$. The spectrum is weighted using a Gaussian function and then inverse transformed into the time domain using the FFT. The result is shown in Figure 4. This time-domain reflection coefficient consists of a sequence of pulses arising from reflections at the air/material and conductor interfaces. Unlike in the case of a lossless uniform dielectric layer, the pulses are not duplicates of the Gaussian excitation pulse, but are distorted by

the spatial variation in the permittivity. The natural frequencies $\{s_k\}$ are then calculated by solving (63) using collocation. The results for the first ten modes are shown in Table 1. About 200 pulse functions are required to compute the natural frequencies to 5 digits for the lowest order mode, while 1200 functions are required for the tenth mode. It is seen that the frequencies behave very much like those of a uniform layer (72) as the order increases. Similarly, the coupling coefficients $\{c_k\}$ are found from (69) and are also shown in Table 1. Finally, the natural resonance representation of the reflection coefficient is calculated from (65), with $w(s) = 0$, in the frequency range 0.01–20.48 GHz at 2048 points, using the first twelve modes, and the spectrum weighted using the same Gaussian function as previously. The time-domain reflection coefficient found using the FFT is shown in Figure 4. It is seen that the natural mode series matches the inverse transform of the frequency-domain reflection coefficient, except for the initial reflection from the air/material interface (the early time of the response). The discrepancy results from not including the entire function $w(s)$.

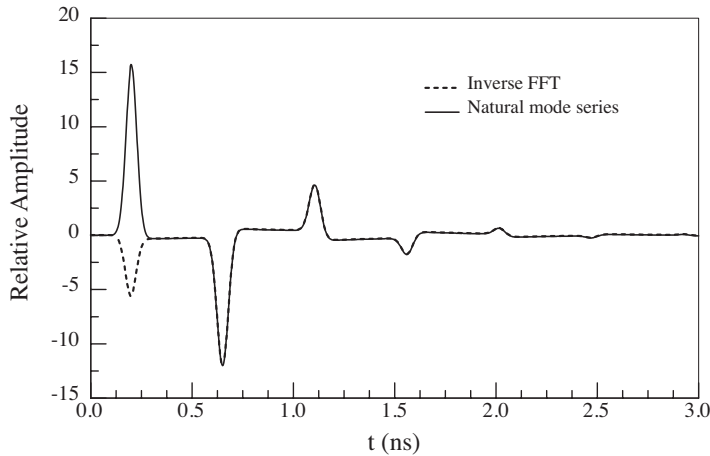
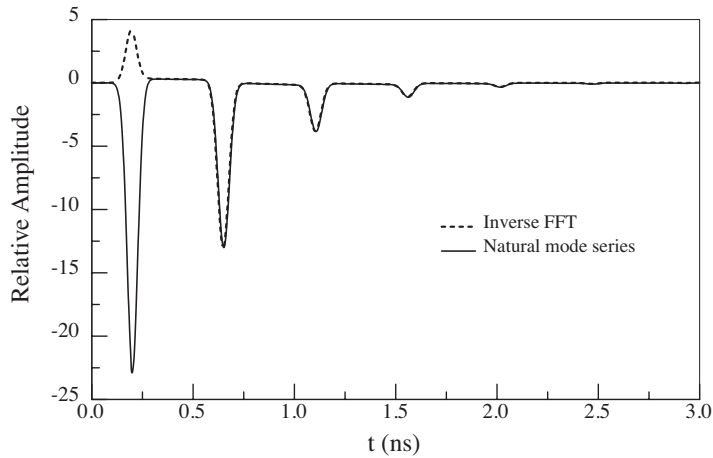


Figure 4. Reflected transient field resulting from Gaussian-pulse excitation of a conductor-backed layer with exponential permittivity profile.

As a final example, consider a conductor-backed layer of thickness 0.03 m with zero conductivity, unit relative permittivity, and a frequency-independent exponential permeability profile (27), where $\mu_{r0} = 4$ and $\kappa = 20$. Proceeding as in the second example above, the reflection coefficient is computed analytically with $\phi_0 = 30^\circ$, and inverse transformed to produce the result is shown in Figure 5. In

Table 1. Natural frequencies of a conductor-backed slab with exponential permittivity profile.

n	s_n (1/s)	c_n (1/s)
0	$-1.938 \times 10^9 + j7.392 \times 10^9$	$4.409 \times 10^9 - j0.2676 \times 10^9$
1	$-2.085 \times 10^9 + j20.87 \times 10^9$	$4.816 \times 10^9 - j0.1936 \times 10^9$
2	$-2.101 \times 10^9 + j34.58 \times 10^9$	$4.871 \times 10^9 - j0.1255 \times 10^9$
3	$-2.106 \times 10^9 + j48.33 \times 10^9$	$4.888 \times 10^9 - j0.0917 \times 10^9$
4	$-2.108 \times 10^9 + j62.10 \times 10^9$	$4.894 \times 10^9 - j0.0720 \times 10^9$
5	$-2.109 \times 10^9 + j75.87 \times 10^9$	$4.898 \times 10^9 - j0.0592 \times 10^9$
6	$-2.110 \times 10^9 + j89.64 \times 10^9$	$4.900 \times 10^9 - j0.0502 \times 10^9$
7	$-2.110 \times 10^9 + j103.4 \times 10^9$	$4.901 \times 10^9 - j0.0436 \times 10^9$
8	$-2.110 \times 10^9 + j117.2 \times 10^9$	$4.902 \times 10^9 - j0.0385 \times 10^9$
9	$-2.111 \times 10^9 + j131.0 \times 10^9$	$4.903 \times 10^9 - j0.0345 \times 10^9$

**Figure 5.** Reflected transient field resulting from Gaussian-pulse excitation of a conductor-backed layer with exponential permeability profile.

contrast to the reflections from the layer with exponential permittivity profile, each of the multiple reflections has the same sign, rather than alternating. Next, the natural frequencies $\{s_k\}$ are calculated by solving (63). Here, the natural mode expansion (59) is substituted into the integral equation (51), and the matrix entries are determined through collocation. The results for the first ten modes are shown

in Table 2. Note that the imaginary part of the first frequency is zero, and that the frequencies behave very much like those of a layer of uniform permeability (73) as the order increases. Again, the coupling coefficients $\{c_k\}$ are found from (69) and are also shown in Table 2. Finally, the natural resonance representation of the reflection coefficient is calculated from (65), with $w(s) = 0$. The time-domain reflection coefficient found using the natural mode series is shown in Figure 5. It is seen that the natural mode series matches the inverse transform of the frequency-domain reflection coefficient, except for the initial reflection from the air/material interface (the early time of the response), a result of not including the entire function $w(s)$.

Table 2. Natural frequencies of a conductor-backed slab with exponential permeability profile.

n	s_n (1/s)	c_n (1/s)
0	$-2.330 \times 10^9 + j0.000 \times 10^9$	$-5.747 \times 10^9 + j0.0000 \times 10^9$
1	$-2.727 \times 10^9 + j13.92 \times 10^9$	$-6.893 \times 10^9 + j0.4933 \times 10^9$
2	$-2.759 \times 10^9 + j27.64 \times 10^9$	$-7.065 \times 10^9 + j0.2873 \times 10^9$
3	$-2.765 \times 10^9 + j41.40 \times 10^9$	$-7.103 \times 10^9 + j0.1976 \times 10^9$
4	$-2.767 \times 10^9 + j55.17 \times 10^9$	$-7.117 \times 10^9 + j0.1499 \times 10^9$
5	$-2.768 \times 10^9 + j68.95 \times 10^9$	$-7.123 \times 10^9 + j0.1205 \times 10^9$
6	$-2.769 \times 10^9 + j82.72 \times 10^9$	$-7.127 \times 10^9 + j0.1007 \times 10^9$
7	$-2.769 \times 10^9 + j96.50 \times 10^9$	$-7.129 \times 10^9 + j0.08647 \times 10^9$
8	$-2.770 \times 10^9 + j110.3 \times 10^9$	$-7.130 \times 10^9 + j0.07574 \times 10^9$
9	$-2.770 \times 10^9 + j124.1 \times 10^9$	$-7.131 \times 10^9 + j0.06738 \times 10^9$

8. CONCLUSIONS

A natural-mode expansion for the field reflected by a conductor-backed inhomogeneous layer has been presented. The frequency-domain field distribution within the slab is found by solving a differential equation, which may be converted to an integral equation and solved using the method of moments. The natural frequencies of the slab are found by solving a homogeneous integral equation. It is found that the late-time natural-mode response of the slab matches the transient response found by computing the inverse fast Fourier transform of the frequency-domain reflection coefficient. This result should prove useful for diagnosing changes to the material parameters of inhomogeneous layers.

REFERENCES

1. Hashish, E. A., "Forward and inverse scattering from an inhomogeneous dielectric slab," *J. of Electromagn. Waves and Appl.*, Vol. 17, No. 5, 719–736, 2003.
2. Umashankar, K., S. Chaudhuri, and A. Taflove, "Finite-difference time-domain formulation of an inverse scheme for remote sensing of inhomogeneous lossy layered media: Part I – one dimensional case," *J. of Electromagn. Waves and Appl.*, Vol. 17, No. 5, 719–736, 2003.
3. He, S., P. Fuks, and G. W. Larson, "An optimization approach to time-domain electromagnetic inverse problem for a stratified dispersive and dissipative slab," *IEEE Trans. Antennas and Propagat.*, Vol. 44, No. 9, 1277–1282, 1996.
4. Kim, Y., D. L. Jaggard, and N. Cho, "Time-domain inverse scattering using a nonlinear renormalization technique," *J. of Electromagn. Waves and Appl.*, Vol. 4, No. 2, 99–111, 1990.
5. Tijhuis, A., "Iterative determination of permittivity and conductivity profiles of a dielectric slab in the time domain," *IEEE Trans. Antennas and Propagat.*, Vol. 29, No. 2, 239–245, 1981.
6. Bolomey, J.-C., C. Durix, and D. Lesselier "Determination of conductivity profiles by time-domain reflectometry," *IEEE Trans. Antennas and Propagat.*, Vol. 27, No. 2, 244–248, 1979.
7. Stenholm, G., E. J. Rothwell, D. P. Nyquist, L. C. Kempel, and L. L. Frasc, "E-pulse diagnostics of simple layered materials," *IEEE Trans. Antennas and Propagat.*, Vol. 51, No. 12, 3221–3227, 2003.
8. Oh, J., E. J. Rothwell, D. P. Nyquist, and M. J. Havrilla, "Natural resonance representation of the transient field reflected by a conductor-backed lossy layer," *J. of Electromagn. Waves and Appl.*, Vol. 17, No. 5, 673–694, 2003.
9. Oh, J., E. J. Rothwell, B. T. Perry, and M. J. Havrilla, "Natural resonance representation of the transient field reflected by a conductor-backed layer of Debye material," *J. of Electromagn. Waves and Appl.*, Vol. 18, No. 5, 571–589, 2004.
10. Perry, B. T., "Natural resonance representation of the transient field reflected from a multi-layered material," Ph.D. Dissertation, Michigan State University, August 2005.
11. Tijhuis, A. G., "SEM approach to the transient scattering by an inhomogeneous, lossy dielectric slab; Part 2: The inhomogeneous case," *Wave Motion*, Vol. 6, 167–182, 1984.
12. Abramowitz, M. and I. Stegun, *Handbook of Mathematical*

- Functions*, Dover Publications, New York, 1965.
13. Gradshteyn, I. S. and I. M. Ryzhik, *Tables of Integrals, Series, and Products*, Academic Press, London, UK, 1994.
 14. Khalaj-Amirhosseini, M., "Analysis of lossy inhomogeneous planar layers using Taylor's series expansion," *IEEE Trans. Antennas and Propagat.*, Vol. 54, No. 1, 130–135, 2006.
 15. Chew, W., *Waves and Fields in Inhomogeneous Media*, IEEE Press, New York, 1999.
 16. Collin, R. E., *Field Theory of Guided Waves*, IEEE Press, New York, 1990.
 17. Baum, C. E., "The singularity expansion method," *Transient Electromagnetic Fields*, L. B. Felsen (ed.), Springer, Berlin, 1976.